Separation Science and Technology
Publication details, including instructions for authors and subscription information:
http://www.informaworld.com/smpp/title~content=t713708471

Pore Network Modeling of Nanoporous Ceramic Membrane for Hydrogen Separation

Mohammad Moeini[a]; Fatolah Farhadi[a]
[a] Department of Chemical and Petroleum Engineering, Sharif University of Technology, Tehran, Iran

Online publication date: 15 September 2010

To cite this Article Moeini, Mohammad and Farhadi, Fatolah(2010) 'Pore Network Modeling of Nanoporous Ceramic Membrane for Hydrogen Separation', Separation Science and Technology, 45: 14, 2028 — 2038
To link to this Article: DOI: 10.1080/01496395.2010.504437
URL: http://dx.doi.org/10.1080/01496395.2010.504437

Separation Science and Technology, 45: 2028–2038, 2010

ISSN: 0149-6395 print/1520-5754 online
DOI: 10.1080/01496395.2010.504437

Taylor & Francis
Taylor & Francis Group

Pore Network Modeling of Nanoporous Ceramic Membrane for Hydrogen Separation

Mohammad Moeini and Fatolah Farhadi
Department of Chemical and Petroleum Engineering, Sharif University of Technology, Tehran, Iran

Pore network modeling of porous media has this advantage that can consider the pore structure incorporating any desired details, but it has not been studied sufficiently. In addition, most studies are limited to mathematical modeling only which need validation. In the present study, this approach was applied to hydrogen separation from syngas by nanoporous ceramic membrane to predict the membrane permeance theoretically based on its pore structure. Gas transport through nanoporous membrane was modeled with the aim of a 2D network model. A dusty gas model was used for gas transport in the individual pores. Model validation showed that the model predictions are in good agreement with the experimental data with the coordination number of 2.5 and the pore length of about 20 nm. A parametric study indicated that hydrogen permeance through the membrane increases with the average and minimum pore size and decreases with temperature and pressure. Also, hydrogen selectivity increases slightly with temperature and decreases with pressure and average pore size.

Keywords dusty gas model; hydrogen; nanoporous membrane; network modeling; syngas

INTRODUCTION

Hydrogen has been considered as an attractive alternative to the fossil sources in recent years, because when it is used in a fuel cell or internal combustion engine, it results in a near pollution-free energy with water as the main by-product (1). Hydrogen also is used extensively in many industrial sectors, such as refining, petrochemical, ammonia synthesis, metallurgy, and semi-conductors (2,3). The hydrogen usage is expected to increase in the future by the development of fuel cell applications. Another advantage of hydrogen is its flexibility. ''While fossil sources are limited to specific geographical areas, localized production of hydrogen is feasible nearly everywhere from several sources (fossil fuels, biomass, water, etc.)'' (1).

Currently, steam reforming of natural gas is the main process for hydrogen production. Thus, the separation of hydrogen from syngas is an important separation process. The membrane methods of separation have been considered as an attractive alternative to the conventional separation processes because of their lower capital costs and greatly reduced energy consumption. Elimination of all process heat requirements, cleaner and safer mode of operation, and the lack of mechanical complexity are other advantages of membrane separation processes (4–8).

There are different categories of H_2 separation membranes, such as, dense or nonporous metal membranes, nanoporous inorganic membranes, and polymeric membranes. Polymeric membranes are not suitable for syngas separation due to their limited stability at high temperatures. Nanoporous membranes offer many advantages over dense membranes. More importantly, while the flux is directly proportional to the pressure in porous membranes, it is proportional to the square root of the pressure in dense metal membranes. Therefore, porous membranes are the more attractive option for operation at high pressures. Moreover, porous membranes are cheaper than dense metal membranes, because dense metal membranes usually are made from Pd and its alloys which are expensive (4,9).

Ceramic and carbon membranes are two common types of nanoporous membranes which are used in hydrogen separation (4). The disadvantage of carbon membranes is that they are brittle and can be difficult to package if a large membrane surface is needed. Furthermore, carbon membranes are still expensive (4,9). Ceramic membranes are more suitable for syngas separation, because they have higher chemical, mechanical, and thermal stability which are essential for syngas separation at high pressure and temperature (10).

Considerable development has been made in the controlled synthesis of nanoporous materials in the recent years. The structure of porous materials can be controlled on two levels:

1. in macroporous structure level, by mixing of particles with different sizes, and then, specific thermal treatment, and
2. in mesoporous and microporous structure level, by the use of specific material of particles with specific mesoporous or microporous structure (11).

Received 3 May 2009; accepted 20 April 2010.
Address correspondence to Fatolah Farhadi, Department of Chemical and Petroleum Engineering, Sharif University of Technology, Azadi Ave., Tehran, Iran. Fax: +982166022853. E-mail: farhadi@sharif.edu

The modeling of gas transport through membranes can be a useful tool in finding the optimum porous structure (porosity, tortuosity, pore size distribution, pore's shape, etc.) and improve the separation properties of the membrane with controlling its structure during the fabrication process. While there are a lot of papers on the fabrication and characterization of nanoporous membranes, studies on transport mechanisms through them and modeling their nanoporous structure are limited.

GAS TRANSPORT THROUGH POROUS MEMBRANE

Different approaches have been developed to model transport through porous media, but they can be divided into four general categories:

1. statistical models,
2. geometrical models,
3. corrected averaged form of governing differential equations, and
4. dusty gas model.

The main difference between these approaches lies in the way they deal with the random structure of porous media.

Since a porous medium is generally a random structure, the idea of developing statistical models is appealing. "Whenever a probability law is used in the model, the term statistical model seems appropriate" (12). Two kinds of these models are cut-and-random-rejoin-type model, which was introduced by Childs and Collis-George (13), and the model of Haring and Greenkorn (14).

In geometric models, a specific geometry which hopefully is to some extent similar to the porous medium is considered. There are different kinds of geometric models, such as one-dimensional models, Bethe lattice models, and network models.

In one-dimensional models the pore space is considered to be made of a bundle of parallel capillary tubes, or a collection of tubes in series. The disadvantage of one-dimensional models is that they cannot take into account the interconnectivity of the pores, the existence of pore loops, etc. As a result, many predictions of such models are grossly in error, and they are so simple that they cannot be improved (15).

Deriving the analytical formulae for the properties of interest is often possible with Bethe lattice models, and sometimes, the predictions of such formulae are well in agreement with those of three-dimensional systems. One of the disadvantages of these models is that they cannot take into account the closed loop of bonds, which are a major element of the topology of real pore spaces (15).

"Models of pore structure, consisting of three-dimensional networks where the pore sizes are distributed over the bonds and/or the nodes of the network in a disordered manner, come to resemble closest the structure of real porous media" (12). Different networks have been considered, such as square, trigonal, hexagonal, kagome, and crossed square.

The third approach is the development of correct averaged forms of the governing differential equations. These equations should be valid for any geometry, thus the results obtained for specific geometric models must satisfy the averaged equations. In addition, any statistical model should be in accord with the averaged equations (16).

Another distinct approach is the "dusty gas model" (17) which describes the porous material as a number of large particles with zero velocity which are dispersed throughout the gas mixture. The disadvantage of this model is that it avoids any assumption about the exact internal structure of the porous material. Therefore, averaged empirical and semi-empirical factors such as the porosity and tortuosity of the porous material are required.

The above discussion shows that network modeling is the only approach which is capable of considering the internal structure of porous media incorporating any desired details. Moreover, this model can take into account the interconnectivity of pores and the closed loop of bonds. Despite their importance, network models have not been studied sufficiently because of their high computational load. In addition, most of these studies are theoretical modeling only which need validation with the experimental data. Thus, the present study aims to apply this modeling approach to hydrogen separation from syngas by nanoporous ceramic membrane which is a highly important separation process in the fuel cell applications. Syngas mixture transport through the nanoporous membrane has been modeled via network modeling to obtain membrane permeance and selectivity theoretically, based on the considered pore structure. The developed model then has been validated by two sets of experimental data. This validation is one of the significant features of this study, because there are limited articles on both network modeling and its validation.

MODELING

While the dusty gas model cannot include the exact internal structure of porous media, it results in analytical equations for transport through simple and specific geometries, such as capillary tubes, and these equations do not require any empirical constant. In addition, this model gives a strong theoretical basis for combining different transport mechanisms. Thus, the pore structure is modeled via a two-dimensional network model and the dusty gas model is used for modeling the transport through each bond, and not for transport through the entire membrane.

Pore Network Description

In this study, the nanoporous membrane is represented by a two-dimensional square network. In this network, the bonds represent the pore throats or the narrow channels that connect the sites which represent the pore bodies (Fig. 1). Pores' volume can be assigned to bonds, sites, or both of them, but in most cases the sites are ignored and no volume is assigned to them (15). In the present study, the sites have been ignored and the pores' volume has been assigned to the bonds. The bonds are assumed as cylinders with a smooth internal surface which have similar length. The effective radius of each bond is selected from the below pore size distribution (PSD) which is similar to the experimental PSD for many membranes (18):

$$f(r) = \frac{r - r_m}{(r_a - r_m)^2} \exp\left[-\frac{1}{2}\left(\frac{r - r_m}{r_a - r_m}\right)^2\right] \tag{1}$$

r_a and r_m are average and minimum pore radius, respectively, and can be selected from experimental PSDs.

To make the network similar to real pore structure, some of the pores are removed randomly. In this way, the average coordination number (number of bonds which are connected to each node) becomes less than 4 (19):

$$P_b = 1 - \frac{1}{4} Z_p \tag{2}$$

where Z_p is average coordination number and P_b is the fraction of pores which has been removed.

Multicomponent Gas Transport in the Pores

As said, the dusty gas model is used for modeling the gas mixture transport through individual pores. "In this model, the porous medium is treated as one component of the gas mixture, consisting of giant molecules held fixed in space, and the highly developed kinetic theory of gases is applied to this supermixture" (17). This model considers three modes of gas transport:

1. free-molecule or Knudsen flow,
2. continuum or ordinary diffusion, and
3. viscous flow.

The development of transport equations is very complicated and requires many equations from the kinetic theory of gases. Thus, only the final results are presented here:

$$\mathbf{J}_D = -\mathbf{D}\frac{d\mathbf{C}}{dz} \tag{3}$$

$$\mathbf{J}_{visc} = -\frac{B_0 Z R T \mathbf{C}}{\eta}\frac{dC}{dz} \tag{4}$$

where $\mathbf{C}$ is the concentration, C is the total concentration, $\mathbf{J}_D$ is the diffusive flux (containing Knudsen and continuum diffusion), and $\mathbf{J}_{visc}$ is the viscous flux. B_0, the viscous flow parameter, is a constant characteristic of the pore geometry, and the inverse of matrix $\mathbf{D}$ ($\mathbf{D}^{-1} = [D_{ij}]^{-1} = [a_{ij}]$) is defined as below:

$$a_{ij} = \begin{cases} -\frac{x_j}{D_i\left(\frac{\varepsilon}{q}\right)} & i \neq j \\ -\frac{1}{D_{iK}\left(\frac{\varepsilon}{q}\right)} + \sum\limits_{\substack{k=1 \\ k\neq i}}^{\nu} \frac{x_k}{D_k\left(\frac{\varepsilon}{q}\right)} & i = j \end{cases} \tag{5}$$

D_i is hindered diffusivity, D_{iK} is Knudsen diffusivity, and ϵ/q, the porosity-tortuosity factor, is a constant related to the pore geometry. It was mentioned that pores are assumed as capillary cylindrical tubes, so $B_0 = \frac{r^2}{8}$ and $\frac{\varepsilon}{q} = 1$ (17). Total flux is given by:

$$\mathbf{J} = \mathbf{J}_{visc} + \mathbf{J}_D \tag{6}$$

While Chapman-Enskog theory yields an exact equation for computing the Knudsen diffusivity, this equation is very complicated and not suitable for application in the network model. What is important in this exact equation is that the Knudsen diffusivity is proportional to $(T/M_i)^{1/2}$ (17). In practice, other parameters must be obtained experimentally. Thus it is recommended to use the simple equations which follow the above relationship. The following equation, which is the exact equation for Knudsen diffusivity in infinitely long cylindrical pore, can approximate Knudsen diffusivity in a finite capillary tube (10):

$$D_{iK} = \frac{4}{3} r \sqrt{\frac{2RT}{\pi M_i}} \tag{7}$$

where r is the pore radius. The hindered diffusivity is given by (18):

$$D_i = D_i^{\infty} h(\lambda) \tag{8}$$

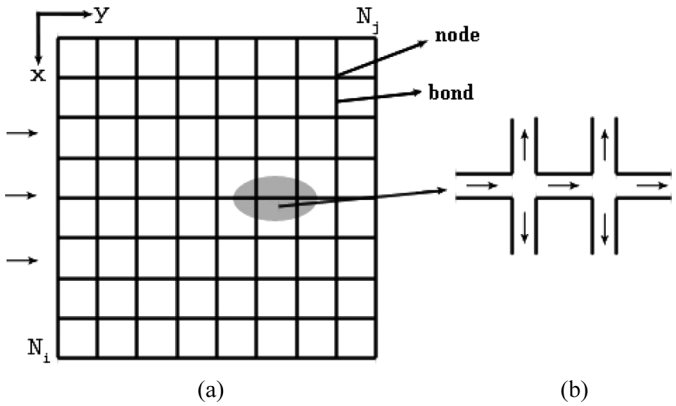

FIG. 1. Square network with the coordination number of 4 (a) network description (b) transport in the bonds and nodes.

$\lambda = R_i/r$, with R_i being the molecular size of gas i, D_i^{∞} is the bulk diffusivity, and $h(\lambda)$ is a function that modifies the bulk diffusivity for diffusion in the pore:

$$h(\lambda) = (1-\lambda)^2(1 - 2.104\lambda + 2.09\lambda^3 - 0.95\lambda^5) \quad (9)$$

Governing Equations

With steady state assumption in each pore for all of the components, transport equations in each pore are as below:

$$\frac{dJ_i}{dz} = 0, \quad i = 1, 2, \ldots, \upsilon \quad (10)$$

where J_i is the total flux of component i. Also, at every node j of the pore network, the mass balance for each component of the gaseous mixture must be established:

$$\sum_{k}^{Z_j} S_k J_i^{(k)} = 0, \quad i = 1, 2, \ldots, \upsilon \quad (11)$$

where $J_i^{(k)}$ is the total flux of component i in pore k that reaches node j, S_k is the cross-sectional area of pore k, and Z_j is the coordination number of node j. Equations (10) and (11) govern the transport of gaseous mixture through the nodes and pores of the network which must be solved simultaneously with suitable boundary conditions.

Boundary Conditions

For the feed side of the membrane, the boundary conditions are:

$$C_i = C_{fi} \quad i = 1, 2, \ldots, \upsilon \quad (12)$$

where C_{fi} is the feed side concentration of component i. If a sweep gas is used in the permeate side, the boundary condition is as below for there:

$$C_i = 0 \quad i = 1, 2, \ldots, \upsilon \quad (13)$$

For the other surfaces, no-flux boundary condition is used (18).

SOLUTION PROCEDURE

Equations (10) and (11) form a differential equations system. Since the second-order differential equations for each pore must be solved with their own boundary conditions, it seems that the finite difference method is the best choice for solving the governing equations system. By using the finite difference method, the differential equations system is converted to a nonlinear algebraic equations system which must be solved with an efficient method. Newton's method (20) with variable step size has been used for this purpose. The golden section method (21), which is an optimization method, has been used to find the optimum step size.

RESULTS AND DISCUSSION

Model Validation

The developed model is validated by two different experimental data sets of Araki et al. (22) and Yoshino et al. (23). The specifications of the membranes which have been used in these references are given in Table 1. For the purpose of modeling, the effect of support and intermediate layers is neglected compared to the selective layer. It is assumed that support and intermediate layers have no serious effect on the permeance of gases through the membrane and the separation performance. Real values of the average pore diameter and membrane thickness are used for network generation, while the coordination number and number of nodes in the transport direction are tuned to make the model a better representation of the real membrane. A comparison of model results with the experimental data showed that the model predictions are in good agreement with the experimental data when the coordination number and pore length are 2.5 and about 20 nm, respectively (Figs. 2 and 3). Permeance is defined as the

TABLE 1
The specifications of nanoporous membranes for model validation

Membrane	Description	Reference
Membrane 1	Support: α-alumina Thickness: 2 mm, Average pore diameter: 0.15 μm, Porosity: 0.4 Selective layer: γ-alumina Thickness: 400 nm, Average pore diameter: 4.4 nm	Araki et al. (22)
Membrane 2	Support: α-alumina Thickness: 1 mm, Average pore diameter: 0.7 μm, Porosity: 0.4 Intermediate layer: α-alumina Thickness: 65 μm, Average pore diameter: 60 nm, Porosity: 0.39 Selective layer: γ-alumina Thickness: about 300 nm, Average pore diameter: 4.3 nm	Yoshino et al. (23)

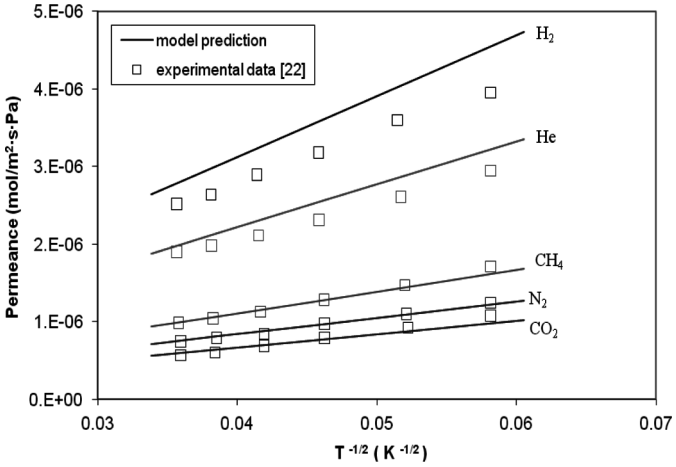

FIG. 2. Comparison of model results with the experimental data (22) (average pore diameter: 4 nm, minimum pore diameter: 0, membrane thickness: 400 nm, average coordination number: 2.5).

ratio of flux over partial pressure difference across the membrane:

$$Q_i = \frac{J_i}{\Delta P_i} \tag{14}$$

It is observed that the temperature dependency of the permeance and the order of the permeance of components are predicted completely correct, and more importantly, the predicted permeance values are in good agreement with the experimental data. It should be mentioned that the most important objective of this study is to calculate the permeance of a real nanoporous membrane based on the available information on its pore structure (i.e., its pore size distribution and selective layer thickness and porosity), and model validation showed that the developed model successfully does this. Good prediction of this two-dimensional pore network model shows that for some applications it is not really necessary to use three-dimensional networks with heavier computational load.

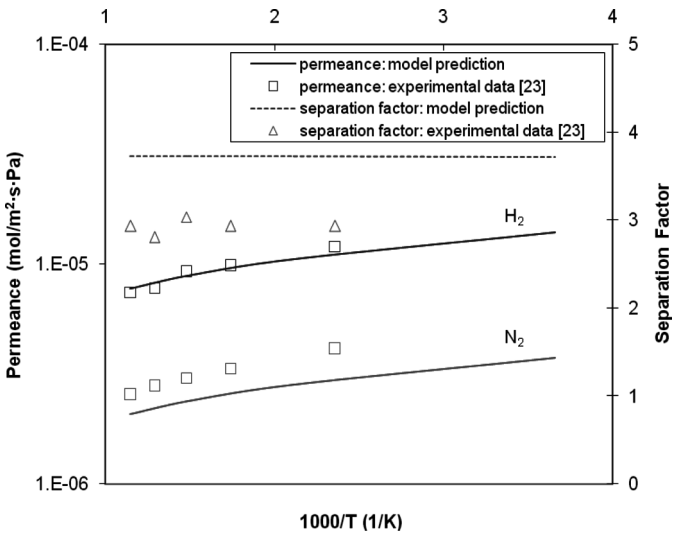

FIG. 3. Comparison of model results with the experimental data (23) (average pore diameter: 4.3 nm, minimum pore diameter: 0, membrane thickness: 300 nm, average coordination number: 2.5).

It may be questioned whether simulated values of 2.5 and 20 nm for the coordination number and pore length agree with what could be inferred from electron micrographs. It should be noticed that square networks are ideal and relatively simple networks. In addition, we have made an assumption which influences these parameters significantly: the sites have been ignored and the volume of the pores has been assigned to the bonds. So, while square network models are a step forward toward the exact modeling of the pore structure and we need to consider more aspects of the pore structure compared to the continuum or one-dimensional models, they are still far from reality. The two-dimensional aspect of the model also influences these values. So, we cannot expect the presented model to predict real pore length and connectivity values. It may be better to see these two parameters as model adjustment parameters. The more important parameter which should have a reasonable value is the porosity of the constructed network (see below).

Model results showed that for membrane 1, the model predictions are more accurate with the average pore diameter of 4 nm, instead of the reported average pore diameter of 4.4 nm in the reference. In the experiments for finding the pore size distribution of porous materials, usually a simple model (e.g., a bundle of capillary tubes) is considered for the pore structure and the pore size distribution is calculated based on the experimental data and this simple structure (12). Thus, the reported PSD is not the real PSD of porous material. It is only an approximation for the real PSD. Since one-dimensional models are very different from the network models, it is not surprising that the network model does not give accurate results with the average pore size calculated from the other models.

As mentioned before, the average coordination number and the number of nodes (or pore length) are two parameters of the developed network model to be adjusted. There are some limitations in adjusting the number of nodes. One of these limitations is the porosity. The constructed square network must have a reasonable porosity. In addition, we have an important constraint—the porosity can not be very close to unity. In practice, the porosity is usually between 30 to 50% for the support and this value is even smaller for the selective layer of the membrane. Increasing the nodes of the network over some value (at constant membrane thickness), causes to have porosity larger than unity which is impossible. Since the porosity of the membrane selective layer has not been reported for the used experimental data, it is not possible to fix the porosity

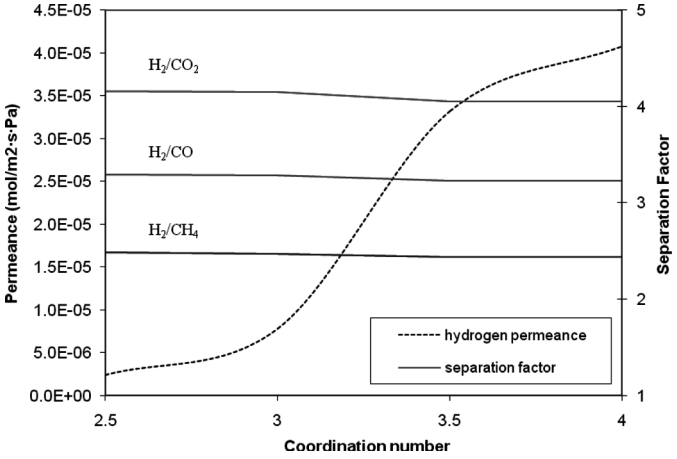

FIG. 4. The effect of average coordination number on the model results (average pore diameter: 4 nm, minimum pore diameter: 0, membrane thickness: 400 nm, feed side pressure: 17 bar, temperature: 750°C, feed composition: 79.6% H_2, 3.1% CH_4, 6.6% CO, 10.7% CO_2).

of the constructed network. But, those combinations of pore length and coordination number are tried that give a reasonable value for the porosity. Figure 4 shows that the average coordination number is a good parameter for model adjustment, because this parameter changes the permeance of components through the membrane, but has no serious effect on the selectivity which determines the separation performance.

One important issue in the network modeling is constructing the network. The goal is to make a random network with the specific size, average coordination number, and PSD, but there are many different random structures with the same size, average coordination number, and PSD. Thus, if the results should be independent of the nature of random structure generation, several realizations of the desired network are to be generated, and the results should be averaged over them. One appropriate approach for this purpose is Monte Carlo simulation. To make this concept clearer, five random networks with the same specifications (all with similar size, average coordination number, and PSD) are shown in Fig. 5. Model results corresponding to these networks are shown in Fig. 6. In Fig. 5, the thickness of bonds shows the pore radius, qualitatively. It is evident from Fig. 6 that the permeance changes a bit from one network realization to another, but the selectivity values are constant for all networks. In the present study, the selective layer of the membrane is very thin and the number of pores in the transport direction is small. So, a little alteration in the network structure can cause a sensible change in the permeance. For large networks however, permeance likely does not change too much from one realization to another. So, this issue is more critical for small networks.

Syngas Separation

Syngas composition depends on the process from which it is produced and the type of feed used. Table 2 summarizes the specifications of syngas produced from six different processes, and Fig. 7 shows the model results for theses syngas streams. The last column in Table 2 is related to the syngas produced in the hydrogen unit of a refinery. In this unit, hydrogen is produced via the steam reforming of a mixture of methane and hydrogen. It is observed that the permeance of components is almost constant for all cases, that is, the permeance of components through the membrane is independent of their feed side mole fraction. This behavior is because of the linear variation of flux with the composition (Fig. 8). Equation (14) indicates that permeance becomes independent of composition when flux varies linearly with the composition.

Parametric Study

In this section, the syngas produced in the hydrogen unit of refinery has been considered for the parametric study.

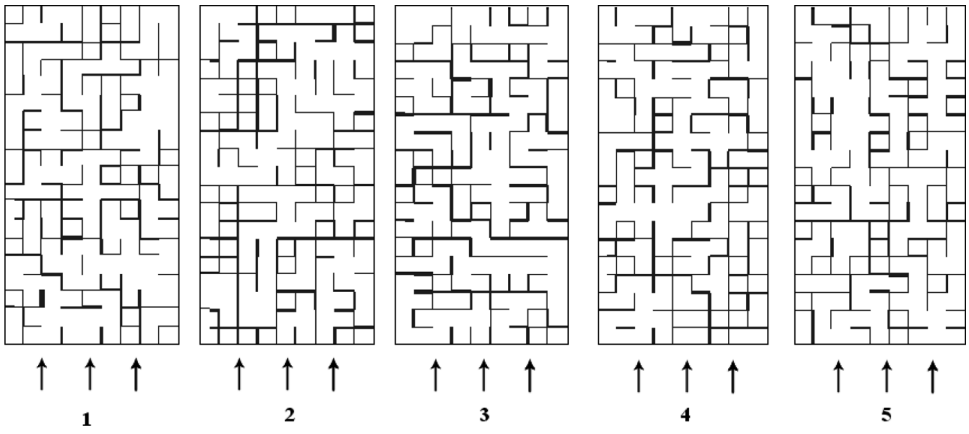

FIG. 5. Five different randomly generated square networks with the same specifications (average pore diameter: 4 nm, minimum pore diameter: 2 nm, membrane thickness: 400 nm, average coordination number: 2.5).

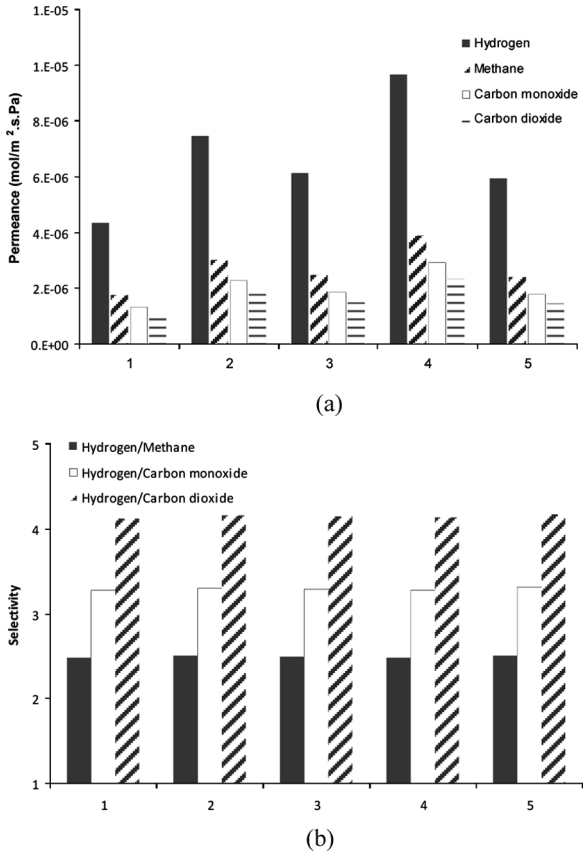

FIG. 6. Model results for the networks shown in Fig. 5 (feed side pressure: 17 bar, temperature: 750°C, feed composition: 79.6% H_2, 3.1% CH_4, 6.6% CO, 10.7% CO_2): (a) permeance values (b) selectivity values.

Figure 9 shows that increasing the average pore size decreases the selectivity and increases the permeance. It is noticed that the average pore size has a considerable effect on the selectivity. In the average pore diameter of 4 nm, selectivity is 4.2, 3.3, and 2.5 for H_2/CH_4, H_2/CO, and H_2/CO_2, while the theoretical Knudsen selectivity values (31) are 4.7, 3.7, and 2.8, respectively. The closeness of selectivity values in the average pore diameter of 4 nm to Knudsen selectivities indicates that Knudsen diffusion is the dominant mechanism in this average pore size. Decrease in the selectivity with the average pore size is due to the increased share of viscous flow mechanism.

Increase in the minimum pore size increases the hydrogen permeance, but has no considerable effect on the selectivity (Fig. 10). Increasing the minimum pore size (r_m) in Eq. (1), while the average pore size (r_a) is fixed, increases the number of pores with the size close to the average pore size, and decreases the pores with very small sizes. This change in the PSD increases the permeance.

Though hydrogen flux through dense palladium membranes increases with temperature (3,29,32), but for nanoporous membranes the trend is reverse (22,23), because transport mechanism is completely different. Our modeling results show this behavior as well (Fig. 11). In our parametric study, the pressure difference across the membrane is fixed. If flux equations (Eqs. (3) and (4)) are written in the form of the pressure gradient instead of the concentration gradient, it will be revealed that the temperature reduces both viscous and diffusive fluxes. Of course, the effect of temperature is greater on the viscous flux. Thus, selectivity increases with temperature due to the increased share of diffusion mechanism compared to viscous flow at higher temperatures (Fig. 11). Readers may be confused as to why does temperature reduce the diffusive flux, while it increases the mobility of molecules? The answer is that while temperature increases the mobility of molecules and diffusivity values, it reduces the concentration gradient in the case of constant pressure difference across the membrane. The effect of temperature on concentration is greater than its effect on diffusivity values and thus, flux through the membrane is reduced with temperature.

TABLE 2
The specifications of syngas streams produced from various processes

Process	Water-coal slurry gasification	Dry coal gasification	Partial oxidation	Steam reforming	Autothermal	Hydrogen unit of refinery
H_2	27–30%	27–30%	62.6%	65.1%	41%	79.6%
CO	35–45%	62–64%	33.7%	1%	1%	6.6%
CO_2	10–15%	<4%	3.1%	15.5%	15%	10.7%
CH_4	–	–	0.3%	0.2%	–	3.1%
H_2O	15–25%	<4%	–	18.2%	9.5%	–
N_2	–	–	0.3%	–	33.5%	–
H_2S	0.2–1.2%	0.2–1.2%	–	–	–	–
Temperature	About 870°C	About 870°C	780–1400°C	750–900°C	850–1300°C	750°C
Pressure	About 27 atm	About 27 atm	25–80 atm	22–35 atm	20–70 atm	17 bar
Reference	(24)	(24)	(25, 26)	(27, 28, 29, 30)	(28, 30)	

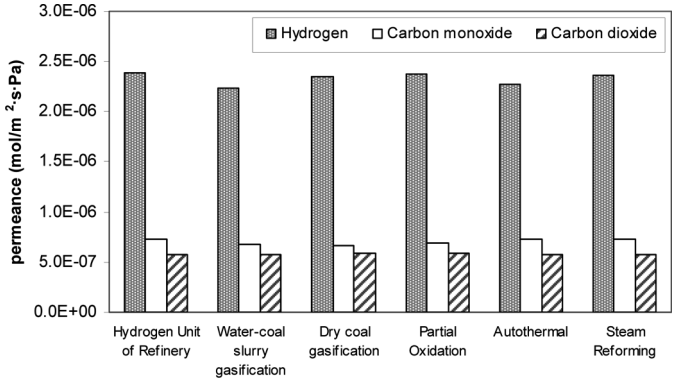

FIG. 7. Model results for various kinds of syngas (average pore diameter: 4 nm, minimum pore diameter: 0, membrane thickness: 400 nm, average coordination number: 2.5, feed side pressure: 17 bar, temperature: 750°C).

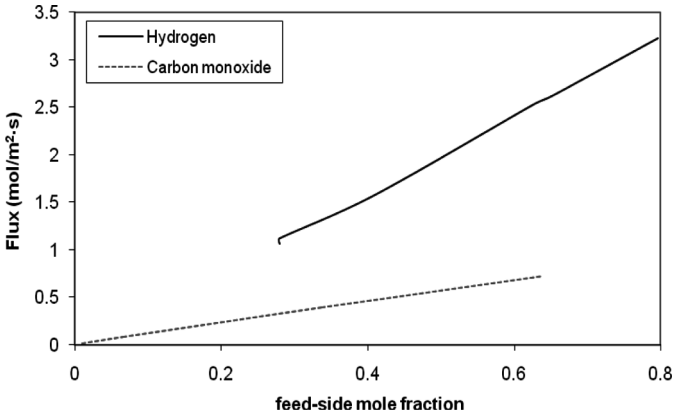

FIG. 8. The effect of feed side mole fraction on the flux (average pore diameter: 4 nm, minimum pore diameter: 0, membrane thickness: 400 nm, average coordination number: 2.5, feed side pressure: 17 bar, temperature: 750°C).

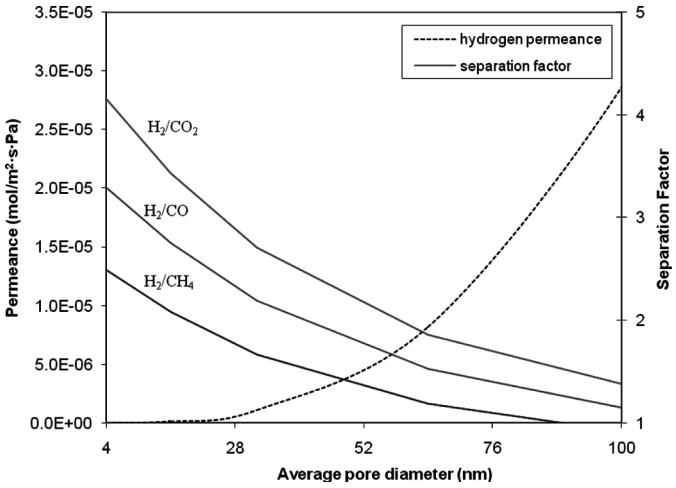

FIG. 9. The effect of average pore diameter on the model results (minimum pore diameter: 0, membrane thickness: 400 nm, average coordination number: 2.5, feed is the steam reforming syngas produced in the hydrogen unit of refinery).

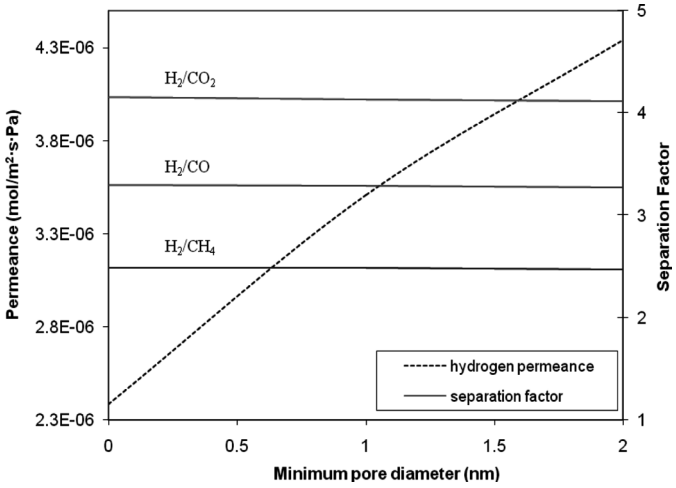

FIG. 10. The effect of minimum pore diameter on the model results (average pore diameter: 4 nm, membrane thickness: 400 nm, average coordination number: 2.5, feed is the steam reforming syngas produced in the hydrogen unit of refinery).

Figure 12 shows that both hydrogen permeance and selectivity decrease with the feed side pressure. Although the flux of hydrogen increases with pressure, the effect of pressure drop increase across the membrane is more than the effect of flux increase, and thus, permeance decreases slightly with pressure (note that permeance is the ratio of flux over partial pressure drop across the membrane). Decrease in the selectivity is due to the increased share of the viscous mechanism at higher pressure drops.

Figure 13 shows the model results for a specific pore structure and operating conditions that seem more suitable

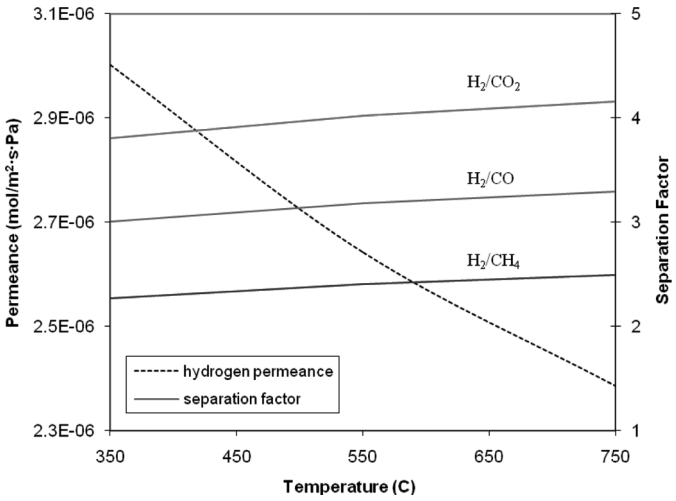

FIG. 11. The effect of temperature on the model results (average pore diameter: 4 nm, minimum pore diameter: 0, membrane thickness: 400 nm, average coordination number: 2.5, feed spec is that of steam reforming syngas produced in the hydrogen unit of refinery).

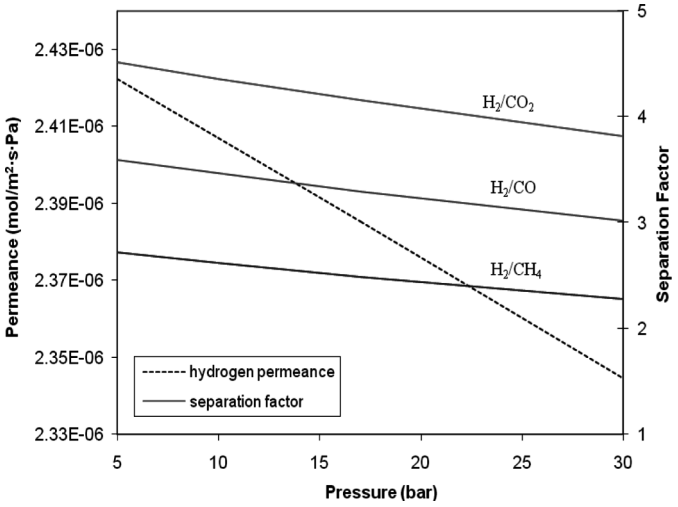

FIG. 12. The effect of feed side pressure on the model results (average pore diameter: 4 nm, minimum pore diameter: 0, membrane thickness: 400 nm, average coordination number: 2.5, temperature: 750°C, feed spec is that of steam reforming syngas produced in the hydrogen unit of refinery).

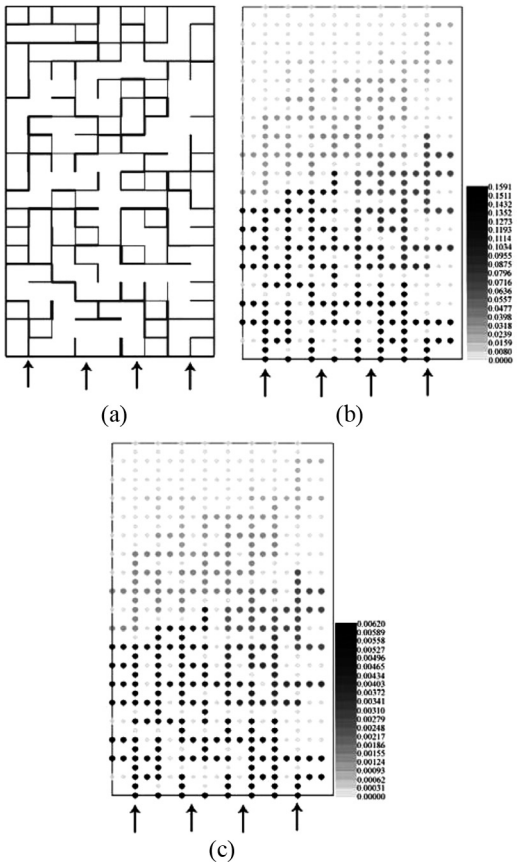

FIG. 13. Model results for a specific pore structure and operating conditions (average pore diameter: 4 nm, minimum pore diameter: 2 nm, membrane thickness: 400 nm, average coordination number: 2.5, feed side pressure: 17 bar, temperature: 750°C, feed composition: 79.6% H_2, 3.1% CH_4, 6.6% CO, 10.7% CO_2): (a) considered pore structure (b) profile of hydrogen concentration in the network (c) profile of methane concentration in the network.

according to the results of parametric study. Figure 13a shows the constructed pore network, while the profile of hydrogen and methane concentration in this network is shown in Figs. 13b and 13c, respectively.

There are many aspects of pore network modeling which need more studies, such as how developed network models can be used for real systems, or how experimental data on pore structure (like porosity, PSD, porous material geometry, and electron micrographs) can be used to generate networks which predict the important transport properties of the porous media accurately and how good are their predictions. This study tried to answer some of these questions and have a contribution to the development of pore network modeling by applying this model to a real nanoporous membrane for an important separation process and validating its predictions. But, more and more studies are required to mature this modeling approach. Different networks (square, triangular, etc.) as well as two and three-dimensional networks should be compared with each other and more validation studies should be performed to confirm that previously developed models are really reliable.

CONCLUSIONS

A two-dimensional random square network model was applied to hydrogen separation from syngas by nanoporous ceramic membrane to predict the membrane permeance theoretically. Model validation with the experimental data on real membranes indicated that the model predictions are in good agreement with the experimental data with the coordination number of 2.5 and the pore length of about 20 nm. Good prediction of the membrane permeance with two-dimensional network suggested that for some applications it is not really necessary to use three-dimensional networks with heavier computational load. Also a study of the permeation of various syngases with different compositions through the membrane showed that permeance is not composition dependent. The modeling of different random pore networks with the same size, average coordination number, and PSD showed that while the permeance values change a bit from one network realization to another, the selectivity values are constant for all cases.

A parametric study showed that hydrogen permeance through the membrane increases with average and minimum pore size and decreases with temperature and pressure. Also, it became clear that hydrogen selectivity increases slightly with temperature and decreases with pressure and average pore size. Of course, it should be mentioned that except the average pore size, selectivity does not change much with other parameters. Because with the assumed average pore size for the parametric study (4 nm) Knudsen diffusion is the predominant transport mechanism, which means that molecules do not interact much with one another. The effect of various parameters

on separation performance showed that a porous membrane with the average pore diameter of 4 nm and minimum pore diameter close to this average diameter (for example 2 nm) has a better performance.

ACKNOWLEDGEMENTS

The authors gratefully acknowledge Dr. B. Dabir from Amirkabir University of Technology for his helpful suggestions.

NOMENCLATURE

B_o	viscous flow parameter [m^2]
C	total concentration [mol/m^3]
C_i	concentration of component i [mol/m^3]
C_{fi}	feed side concentration of component i [mol/m^3]
D_i	hindered diffusivity [m^2/s]
D_{iK}	Knudsen diffusivity [m^2/s]
D_i^{∞}	bulk diffusivity [m^2/s]
J	total flux [$mole/m^2 \cdot s$]
J_D	diffusive flux [$mole/m^2 \cdot s$]
J_{visc}	viscous flux [$mole/m^2 \cdot s$]
M	molecular weight
P_b	fraction of pores which has been removed
P_i	partial pressure of component i [Pa]
Q_i	permeance of component i [$mole/m^2 \cdot s \cdot Pa$]
R	gas constant
R_i	molecular size of gas i [m]
r	pore radius [m]
r_a	average pore radius [m]
r_m	minimum pore radius [m]
S_k	cross-sectional area of pore k [m^2]
T	temperature [K]
x	mole fraction
Z	compressibility factor
Z_j	coordination number of node j
Z_p	average coordination number of network
z	axial coordinate of pores [m]

Greek Symbols

ε/q	porosity-tortuosity factor
η	viscosity [$kg/m \cdot s$]
λ	ratio of molecular radius to pore radius
υ	number of components in gas mixture

REFERENCES

1. Campen, A.; Mondal, K.; Wiltowski, T. (2008) Separation of hydrogen from syngas using a regenerative system. *Int. J. Hydrogen Energy*, 33: 332.
2. Chiappetta, G.; Clarizia, G.; Drioli, E. (2006) Design of an integrated membrane system for a high level hydrogen purification. *Chem. Eng. J.*, 124: 29.
3. Iwuchukwu, I.J.; Sheth, A. (2008) Mathematical modeling of high temperature and high pressure dense membrane separation of hydrogen from gasification. *Chem. Eng. Process.*, 47: 1292.
4. Adhikari, S.; Fernando, S. (2006) Hydrogen membrane separation techniques. *Ind. Eng. Chem. Res.*, 45: 875.
5. Freemantle, M. (2005) Membranes for gas separation. *Chem. Eng. News*, 83: 49.
6. Sridhar, S.; Khan, A.A. (1999) Simulation studies for the separation of propylene and propane by ethylcellulose membrane. *J. Membr. Sci.*, 159: 209.
7. Tiscornia, I.; Irusta, S.; Téllez, C.; Coronas, J.; Santamaría, J. (2008) Separation of propylene/propane mixtures by titanosilicate ETS-10 membranes prepared in one-step seeded hydrothermal synthesis. *J. Membr. Sci.*, 311: 326.
8. Burns, R.L.; Koros, W.J. (2003) Defining the challenges for C_3H_6/C_3H_8 separation using polymeric membranes. *J. Membr. Sci.*, 211: 299.
9. Phair, J.W.; Badwal, S.P.S. (2006) Materials for separation membranes in hydrogen and oxygen production and future power generation. *Sci. Technol. Adv. Mater.*, 7: 792.
10. Li, K. (2007) *Ceramic Membranes for Separation and Reaction*; Wiley: West Sussex, England.
11. Kočí, P.; Štěpánek, F.; Kubíček, M.; Marek, M. (2007) Modelling of micro/nano-scale concentration and temperature gradients in porous supported catalysts. *Chem. Eng. Sci.*, 62: 5380.
12. Dullien, F.A.L. (1992) *Porous Media: Fluid Transport and Pore Structure*; Academic Press Inc.: San Diego, CA.
13. Childs, E.C.; Collis-George, N. (1950) The permeability of porous material. *Proc. R. Soc. London Ser.*, A201: 392.
14. Haring, R.E., Green korn, R.A. (1970) A statistical model of a porous medium with nonuniform pores. *AIChE J.*, 16(3): 477.
15. Sahimi, M. (1995) *Flow and Transport in Porous Media and Fractured Rock*; VCH: Weinheim, Germany.
16. Bowen, D.H.M. (Ed.) (1970) *Flow through Porous Media*; ACS Publications: Washington D. C.
17. Mason, E.A.; Malinauskas, A.P. (1983) *Gas Transport in Porous Media: the Dusty-Gas Model*; Elsevier: Amsterdam, Netherlands.
18. Chen, F.; Mourhatch, R.; Tsotsis, T.T.; Sahimi, M. (2008) Pore network model of transport and separation of binary gas mixtures in nanoporous membranes. *J. Membr. Sci.*, 315: 48.
19. Dadvar, M.; Sahimi, M. (2002) Pore network model of deactivation of immobilized glucose isomerase in packed-bed reactors II: three-dimensional simulation at the particle level. *Chem. Eng. Sci.*, 57: 939.
20. Guo, J.; Shah, D.B.; Talu, O. (2007) Determination of effective diffusivities in commercial single pellets: Effect of water loading. *Ind. Eng. Chem. Res.*, 46: 600.
21. Pedregal, P. (2003) *Introduction to Optimization*; Springer: New York.
22. Araki, S.; Mohri, N.; Yoshimitsu, Y.; Miyake, Y. (2007) Synthesis, characterization and gas permeation properties of a silica membrane prepared by high-pressure chemical vapor deposition. *J. Membr. Sci.*, 290: 138.
23. Yoshino, Y.; Suzuki, T.; Nair, B.N.; Taguchi, H.; Itoh, M. (2005) Development of tubular substrates, silica based membranes and membrane modules for hydrogen separation at high temperature. *J. Membr. Sci.*, 267: 8.
24. Bakker, W. (2004) High temperature corrosion in gasifiers. *Mater. Res.*, 7: 53.
25. Galuszka, J.; Pandey, R.N.; Ahmed, S. (1998) Methane conversion to syngas in a palladium membrane reactor. *Catal. Today*, 46: 83.
26. Hinchliffe, A.B.; Porter, K.E. (1997) Gas Separation Using Membranes. 1. Optimization of the Separation Process Using New Cost Parameters. *Ind. Eng. Chem. Res.*, 36: 821.
27. Yegani, R.; Hirozawa, H.; Teramoto, M.; Himei, H.; Okada, O.; Takigawa, T.; Ohmura, N.; Matsumiya, N.; Matsuyama, H. (2007) Selective separation of CO_2 by using novel facilitated transport membrane at elevated temperatures and pressures. *J. Membr. Sci.*, 291: 157.

28. Huang, J.; El-Azzami, L.; Ho, W.S.W. (2005) Modeling of CO_2-selective water gas shift membrane reactor for fuel cell. *J. Membr. Sci.*, 261: 67.
29. De Falco, M.; Di Paola, L.; Marrelli, L. (2007) Heat transfer and hydrogen permeability in modelling industrial membrane reactors for methane steam reforming. *Int. J. Hydrogen Energy*, 32: 2902.
30. Cheng, X.; Shi, Z.; Glass, N.; Zhang, L.; Zhang, J.; Song, D.; Liu, Z.S.; Wang, H.; Shen, J. (2007) A review of PEM hydrogen fuel cell contamination: Impacts, mechanisms, and mitigation. *J. Power Sources*, 165: 739.
31. Prabhu, A.K.; Oyama, S.T. (2000) Highly hydrogen selective ceramic membranes: application to the transformation of greenhouse gases. *J. Membr. Sci.*, 176: 233.
32. Ling, C.; Sholl, D.S. (2007) Using first-principles calculations to predict surface resistances to H_2 transport through metal alloy membranes. *J. Membr. Sci.*, 303: 162.